

A Low-cost EMF Field Sensor for 5G EMF Exposure Measurements

Erdal Korkmaz¹, Stephan Littel¹, Marco Spirito² and John Bolte^{1,3}

¹Research Group Smart Sensor Systems, The Hague University of Applied Sciences, Delft, the Netherlands, 2628 AL

²Electronics Research Laboratory, Department of Microelectronics, Delft University of Technology, Delft, The Netherlands, 2628 CD

³National Institute for Public Health and the Environment (RIVM), Bilthoven, the Netherlands, 3720 BA

ABSTRACT

A low-cost sensornode is introduced to monitor the 5G EMF exposure in the Netherlands for the four FR1 frequency bands. The sensornode is validated with in-lab measurements both with CW signals as for QAM signals and perform for both cases and for all frequency bands an error less than 1 dB for a dynamic range of 40 dB. This sensor is a follow up of the earlier version of our previously developed sensor and have substantial improvements in terms of linearity, error, and stability.

INTRODUCTION

With the roll out of the 5G communication network, new frequency bands will be deployed, and new protocols will be used. Though, in the Netherlands several indoor and outdoor pilots are running, the roll out of 3.6 GHz and the FR2 bands (> 6 GHz) has yet to start. Although the 5G network is designed to communicate more data in a more targeted way and with less energy than with the 4G network, with increasing data traffic, the total exposure will likely increase. Also, due to other types of data traffic, such as with autonomous vehicles and IoT networks, both the modulation of the signals and the locations from which transmission and reception are made will change and will in any case be more intricate with picocells at a short distance.

The National Institute for Public Health and the Environment of the Netherlands (RIVM) published a report on exposure to 5G in 2020 that states that it is important to keep a close watch for change in exposure and possible biological effects [1]. Due to the advent of IoT, the number of connections has increased over the last few years, facilitating the need for a higher number of devices that can be serviced per base station (BS) with a higher throughput per connection [2]. The increase in number of connections caused an increase in the number of BSs [3], adding to the growing uncertainty and anxiety.

The high variability in the measured exposure observed over time further underlined the need for temporal monitoring. Consequently, new sensors have been developed that can measure these higher frequencies and can be used to inform both public and government bodies of the new 5G RF EMF exposure [4].

Recently low-cost EMF sensors are evaluated for the 5G NR exposure [5-7]. The sensors are either commercially available (off-the-shelf Software Defined radio) or constructed by a research institution. A comparison has been performed in both a Gigahertz Transverse Electro Magnetic (GTEM) cell as well as in-situ near a 5G NR base station. The aim of this study is to improve the sensitivity, accuracy, and the stability of the previously developed sensor [5] for the 5G frequency bands in the Netherlands based on above tests.

MATERIALS AND METHODS

Sensor design

The designed EMF sensor consist of three stacked Printed Circuit Boards (PCB) with off-the-shelf components. The first part is the power unit which consist of batteries and buck/boost converters in order to operate for mobile measurement purposes. The second part is the digital unit (Figure 1.a) consist mainly of a NXP LPC5504 microcontroller with a M33 arm cortex core, SD card, real time clock (Maxim DS1374U), and an Ethernet connection (Wiznet W5500). The third part is the analog

unit (Figure 1.b) which consist of Analog Devices RMS detectors LTC5582 with a dynamic range of 57 dB, three bandpass Surface Acoustic Wave filters for 700 MHz, 1400 MHz, and 2100 MHz band and one lumped element filter for 3600 MHz band. For each frequency band, narrowband planar half-wavelength dipole antennas are designed in-house. The antennas are connected to the analog unit with SMA connectors. The whole sensor is shown in Figure 1c.

The voltage levels from each channel of the RMS power detector are connected to microcontroller to process the data. The microcontroller has a built-in 16 bit Analog to Digital Converter (ADC) with a maximum sample-rate of 2 Msamples per second. The microcontroller has a configured system clock of 96 MHz which is used to feed the arm cortex core and the peripherals. Before this clock enters the ADC it is firstly divided by 8 to obtain an ADC clock of 12 MHz (ADCK). The ADC has a configurable sample rate between 3-131 ADCK cycles. It has been configured to the slowest sample rate with this clock yielding a sample-rate of 91.603 ksamples/s for two reasons. Firstly, a lower sample-rate will pick up less environmental spectral noise, especially from switching converters that operate above the 100 kHz. Secondly, the power detector has been configured with an external filtering capacitor of 100 nF. The accompanying rise and fall times are 3 μ s and 50 μ s. The fall time is a more important characteristic to consider such that the system should not act as a peak detector. 50 μ s fall time corresponds to a 20 kHz signal, falling within the sample-rate of 91.603 ksamples/s while leaving some headroom for oversampling of the signal. Finally, hardware averaging is used to further mitigate variance in the ADC output. For one requested ADC sample 128 samples are averaged in hardware which is the internal sample rate.

Calculations

The converted values are finally processed by microcontroller by means of a look-up table to obtain the power levels in a desired form. In EMF assessment, the electric field intensity levels are generally desired. From basic antenna knowledge [8] the power density is:

$$S = \frac{4\pi P_r}{\lambda^2 G} \quad (1)$$

In which, S is the received power density [W/m^2], P_r is the received power [W], λ is the wavelength in free space, and G is the gain of the antenna. The electric field intensity can be calculated by:

$$S = \frac{E^2}{\eta_0} \quad (2)$$

In which E is the electric field intensity amplitude [V/m], and $\eta_0 = 120\pi$ is the free space impedance [Ω].

Calibration

The sensors were initially calibrated onboard in order to determine the output voltage of the RMS power detector in the used frequency bands as a function of the incident power. Hence, in each separate frequency band, a sinusoidal signal was swept using the network analyser as a signal generator (R&S ZNB40) to obtain a look-up table per frequency band for each sensor. A second calibration procedure will be in the GTEM cell to determine the calibration factors including antenna gain and transmission line losses and mismatches similar as in previous work [5-7]. The GTEM generates a vertically polarized TEM wave, corresponding to the direction of the antennas on the devices under test (DUTs).

Before we perform GTEM calibrations we are interested in performance of the sensor for modulated signals as in real application. As an initial test a QAM-64 modulation will be used due to the available facility in the lab to have an indication of performance with respect to modulated signals. The signal bandwidth of a 5G NR signal is depending on subcarrier spacing (SCS). Within the four frequency bands the bandwidth is varying between 10-100 MHz depending also by the choice of telecom provider.

For this reason, we made a selection for the choice of bandwidth increasing gradually per frequency band (downlink) which is listed in Table 1. Each frequency band is then divided into slots based on the bandwidth, with the intention to visualize frequency dependent error within a band.

The measurement setup consists of a signal source, i.e., a Keysight arbitrary waveform generator (M8190A) configured through Matlab to generate the required 64-QAM modulated signal with configurable bandwidth and center frequencies (see Table 1). Moreover, the signal source provides an output power dynamic range from -73 dBm to -7 dBm. The arbitrary waveform generator has a maximum output power of 0 dBm. QAM-64 is a modulated signal, meaning that the peak-to-average power (PAPR) ratio limits are maximum output power. For QAM-64 the PAPR is about 5.6 dB [9]. The PAPR combined with cable losses, mismatches, insertion losses limit the maximum generated power to -7 dBm for the lowest frequency band up to -14 dBm for the highest frequency band. The output power of the signal source is measured using a Rohde and Schwarz FSW spectrum analyzer and an Agilent E4419B power meter for reference. Consequently, the custom-developed DUT node using an LTC5582 true RMS power detector is tested with 64-QAM modulated signal. Since the Agilent E4419B power sensor below -30 dBm levels was deviating substantially from the generated values only spectrum analyser data is considered as a reference to validate the DUT performance.

RESULTS

The relative error, difference between spectrum analyser and DUT, are depicted in Figure 2 for each frequency band with stepped centre frequencies. For 700 and 1400 MHz bands the discrepancies between different carrier frequencies is mainly caused by the flatness of SAW filters. For the 1400 MHz bands the two carrier frequencies (1462 and 1472 MHz) show small spikes which could be a measurement error. For 2100 and 3600 MHz bands the discrepancies between different carrier frequencies are relatively lower. The flatness of the relative error is here the interesting fact since the offset error is an calibration issue and can be corrected in look-up table with an offset. In all four bands the error will decrease below 1 dB after a second offset calibration over a dynamic range of 40 dB. If we consider the dynamic range within the 3 dB error limit, the dynamic range varies from 52 dB for 3600 MHz band up to 62 dB for 700 MHz band.

CONCLUSIONS

In this study we introduced the design of a low-cost 5G NR EMF sensor for sub-6GHz which can be used to build a local measurement network on a dense grid in the Netherlands. The sensor is initially calibrated with CW signals and then validated for QAM signals. For all frequency bands an error less than 1 dB is obtained for a dynamic range of 40 dB and an error less than 3 dB for a dynamic range between 52-62 dB. The developed sensor is a follow up of the earlier version of our previously developed sensor and have substantial improvements in terms of linearity, error, and stability.

ACKNOWLEDGMENTS

The author would like to thank Gagan Deep Singh from Electronics Research Laboratory, Delft University of Technology, for his help for the measurement setup with modulated signals.

This work is part of the European Union's Horizon Europe research and innovation program under grant agreement No 101057527 (NextGEM). Funded by the European Union. Views and opinions expressed are however those of the authors only and do not necessarily reflect those of the European Union. Neither the European Union nor the granting authority can be held responsible for them.

CAPTIONS

Table 1. Frequency bands (downlink) in Netherlands and the chosen bandwidth with corresponding center frequencies.

5G frequency Band	carrier frequency	Bandwidth
700 MHz band	762 MHz	10 MHz
(758 – 788 MHz)	772 MHz	10 MHz
	782 MHz	10 MHz
1400 MHz band	1462 MHz	20 MHz
(1452 – 1492 MHz)	1472 MHz	20 MHz
	1482 MHz	20 MHz
2100 MHz band	2130 MHz	40 MHz
(2110 – 2170 MHz)	2150 MHz	40 MHz
3600 MHz band*	3550 MHz	100 MHz
(3500 – 3700 MHz)	3650 MHz	100 MHz

* expected frequency range, not yet into service.

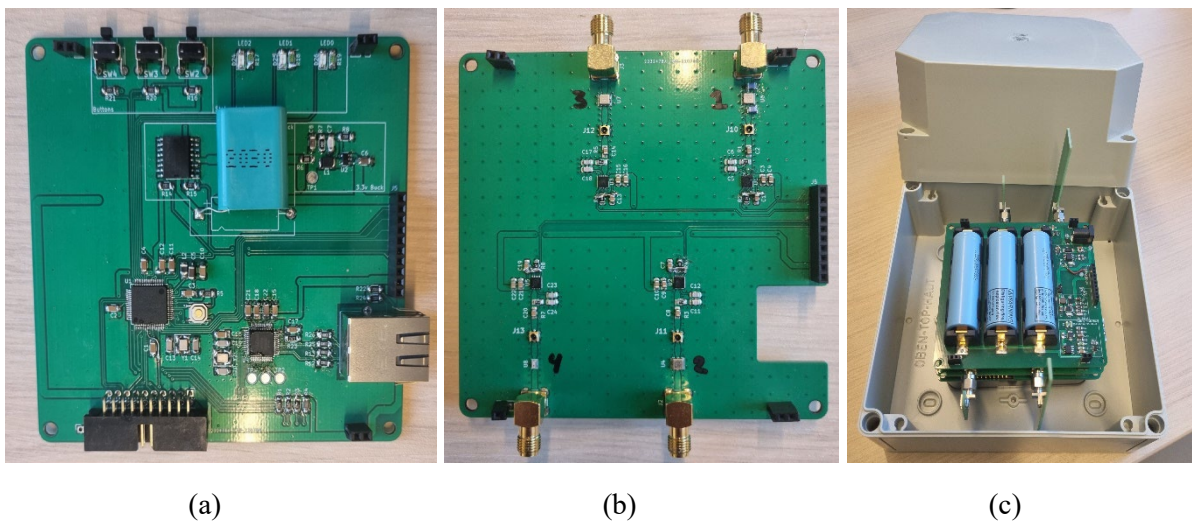


Figure 1: EMF sensor: digital unit (a), analog unit (b), complete sensor with antennas and casing (c).

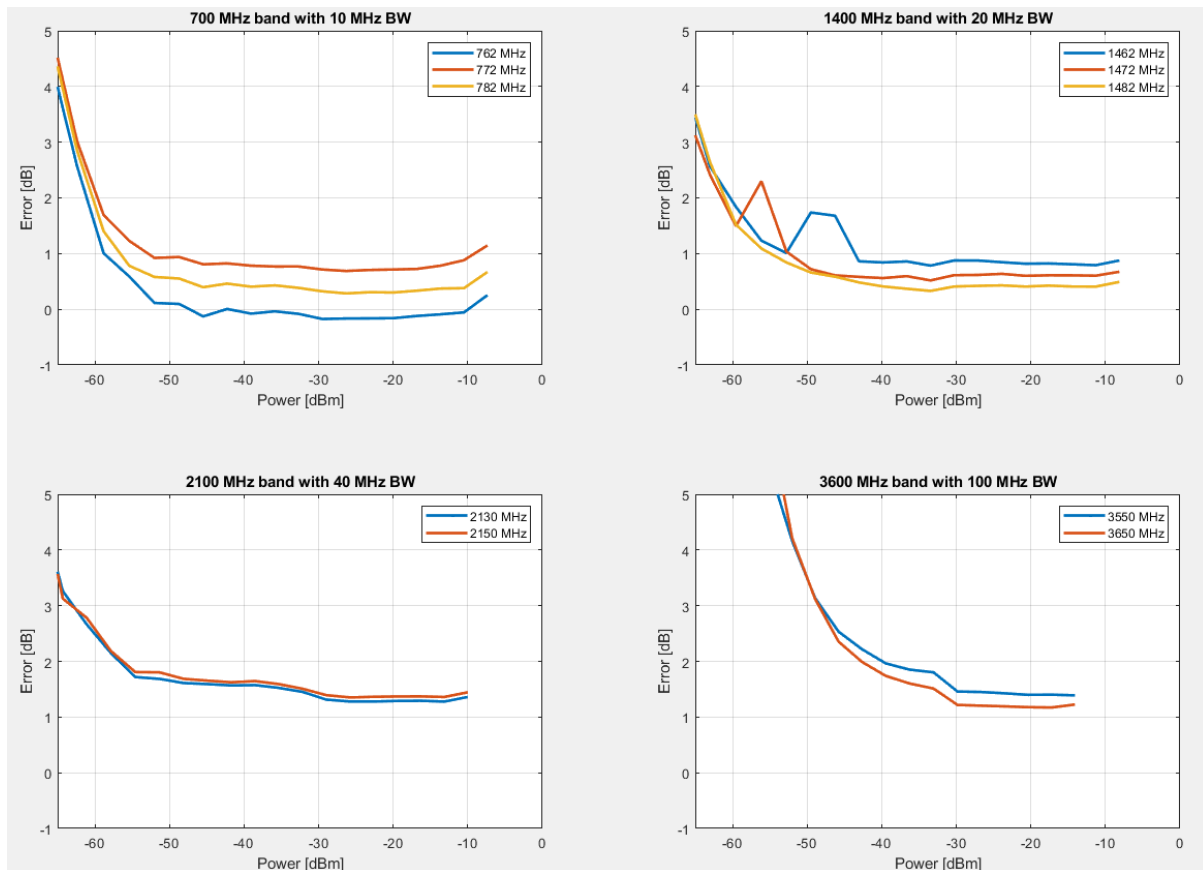


Figure 2: Relative error between DUT and spectrum analyser for each band.

REFERENCES

- [1] R. Stam, J.F.B. Bolte, M.J.M. Pruppers, J. J. Robijns, J. Kamer, L. C. Colussi, “Verkenning van de blootstelling aan elektromagnetische velden afkomstig van 5G-systemen. Small cells en massive MIMO [Exploration of the exposure to electromagnetic fields from 5G systems. Small cells and massive MIMO]”, RIVM en Agentschap Telecom, 2019, RIVM-rapport 2019-0214.
<https://www.rivm.nl/bibliotheek/rapporten/2019-0214.pdf>
- [2] F. Rizzato and I. Fogg, “Quantifying The Impact of 5G and Covid19 on Mobile Data Consumption”, *Internet*, vol. 1, no. 1, pp. 1–15, 2021.
- [3] F. Al-Turjman, E. Ever and H. Zahmatkesh, "Small Cells in the Forthcoming 5G/IoT: Traffic Modelling and Deployment Overview," in *IEEE Communications Surveys & Tutorials*, vol. 21, no. 1, pp. 28-65, Firstquarter 2019, doi: 10.1109/COMST.2018.2864779.
- [4] S. Aerts et al., “Lessons Learned from a Distributed RF-EMF Sensor Network,” *Sensors*, vol. 22, no. 5, p. 1715, Feb. 2022, doi: 10.3390/s22051715.
- [5] E. Korkmaz, S. Littel, J. Bolte, “Development of a low-cost sensor network for measurement of 5G signals in the Netherlands”, *BioEM 2022*, Japan.
- [6] K. Deprez, S. Aerts, A. Thielens, G. Vermeeren, L. Martens, and W. Joseph, “Design of a Low-Cost Modular 5G RF-EMF Exposure Sensor”, *BioEM 2021*, Belgium.
- [7] K. Deprez et al., “Comparison of Low-cost 5G Electromagnetic Field Sensors”, submitted to *BioEM 2023*, Oxford.
- [8] C.A. Balanis, “Antenna Theory: Analysis and Design”. 3rd Edition, John Wiley & Sons, 2005, Chapter 2.
- [9] J. W. Nieto, W. Furman, E. Koski, “Performance Implications of HF Channel Utilization”, *The 10th Nordic Conference on HF Communications*, Sweden, HF13, 2013.